Volume 16, Issue 2, 162504 (1-15)

International Journal of Industrial Chemistry (IJIC)

https://doi.org/10.57647/j.ijic.2025.1604.18

Thermo-Responsive Hydrophobically Associative Terpolymer for Enhanced Oil Recovery: Synthesis, Characterization, and Micromodel Evaluation

Lina Shaheed Ahmed[1], Leila Vafajoo[1,2,*], Ahmad Ramazani Saadatabadi[3,4], Davood Zaarei[1]

[1]*Chemical and Polymer Engineering Department, ST.C., Islamic Azad University, Tehran, Iran*
[2]*Nanotechnology Center, ST.C., Islamic Azad University, Tehran, Iran*
[3]*Chemical and Petroleum Engineering Department, Sharif University of Technology, Tehran, Iran*
[4]*Center for Bioscience & Technology, Institute for Convergence Science & Technology, Sharif University of Technology, Tehran, Iran*

*Corresponding authors: vafajoo@iau.ac.ir, vafajoo@azad.ac.ir

Article History:

Received:
10 November 2025

Revised:
20 December 2025

Accepted:
30 December 2025

Published in Issue:
30 December 2025

Abstract

Polymer flooding represents a key chemical enhanced oil recovery (EOR) technique to improve displacement efficiency in heterogeneous carbonate reservoirs, where residual oil is trapped by capillary forces and early water channeling reduces sweep efficiency. This study evaluates a high-molecular-weight acrylamide-maleic anhydride-styrene terpolymer for EOR in challenging reservoir environments, focusing on its rheological stability, viscoelastic behavior, and displacement performance under controlled micromodel flooding experiments. Micromodels, fabricated from CT scans of carbonate cores to replicate reservoir heterogeneity (porosity 58.97%, average pore radius 14.16 µm, total pore volume 0.230 cm³), were used to assess polymer solutions at concentrations of 500, 750, and 1000 ppm. Experiments varied injection rates (0.005–0.02 mL/min) to examine front stability and sweep efficiency, salinity levels (seawater, 2×SW, 3×SW) to simulate ionic strengths of reservoir brines, and temperatures (25°C, 50°C, 80°C) to evaluate thermal stability and viscosity retention in reservoir-like conditions. Results demonstrate the terpolymer's ability to maintain performance across these parameters, enhancing macroscopic sweep and oil mobilization while addressing limitations of conventional polymers in high-temperature, high-salinity heterogeneous reservoirs.

Keywords: Enhanced Oil Recovery (EOR); Polymer Flooding; Micromodel Testing; Viscoelasticity; Thermal Stability

Cite this article: Shaheed Ahmed L, Vafajoo L, Ramazani Saadatabadi A, Zaarei D. Thermo-Responsive Hydrophobically Associative Terpolymer for Enhanced Oil Recovery: Synthesis, Characterization, and Micromodel Evaluation. Int. J. Ind. Chem., 2025; 16(4):1-15. https://doi.org/10.57647/j.ijic.2025.1604.18

1. Introduction

Polymer flooding is recognized as a promising chemical enhanced oil recovery (EOR) strategy that employs water-soluble macromolecular agents to improve the displacement efficiency of residual crude oil within porous reservoir media [1]. The incorporation of polymer into the injection water markedly increases the solution viscosity, thereby reducing the water–oil mobility ratio and enhancing the macroscopic sweep efficiency [2]. This improvement facilitates the mobilization of capillary-trapped oil by altering the balance between viscous and capillary forces, consequently promoting a more uniform displacement front and mitigating early water channeling during the recovery process [3, 4]. Consequently, the design and optimization of advanced polymeric systems have emerged as a critical area of research in petroleum engineering, aiming to enhance the performance and stability of polymers under diverse reservoir conditions [1, 5]. However, the effectiveness of polymer flooding is

strongly influenced by several factors, including the rheological behavior of the polymer solution, the injection zone characteristics, reservoir permeability heterogeneity, and the contact area of the displacement front within the porous medium [2, 6]. Furthermore, the limitations of polymer flooding in EOR operations primarily arise from the insufficient thermal stability and poor tolerance to high-salinity environments, which can significantly degrade polymer performance under harsh reservoir conditions [7, 8]. Acrylamide-based synthetic polymers are widely utilized in the oil production industry owing to their favorable rheological characteristics, such as high viscosity, shear stability, and tunable molecular architecture, which make them particularly effective for mobility control in polymer flooding operations [9, 10].

It is essential to enhance the physicochemical properties of polyacrylamide-based polymers by developing copolymer systems capable of maintaining stability and performance under dynamic and harsh reservoir conditions, thereby improving oil recovery efficiency [11]. Acrylamide-based polymers structurally modified with hydrophobic monomers have recently attracted significant attention in enhanced oil recovery research [8, 12, 13]. Above a critical aggregation concentration, hydrophobic segments of the polymer chains associate intermolecularly, reinforcing polymolecular interactions and promoting the formation of a three-dimensional network structure [14, 15]. These synthesized block copolymers demonstrate enhanced viscosifying capabilities, which improve sweep efficiency and oil mobilization [16-18]. Consequently, hydrophobically modified copolymers facilitate effective oil displacement while minimizing backflow and preventing the retrapping of oil within pore spaces

Hydrophobically associating polymers and polymeric materials exhibit distinctive physicochemical behaviors under dynamic conditions [19]. This structural feature can help mitigate irreversible mechanical degradation of polymer chains, which often occurs in high-molecular-weight polymers subjected to elevated shear rates [19, 20]. Amphiphilic polymers, such as hydrophobically associating polymers, display synergistic interfacial and rheological properties across diverse systems [21, 22]. Various synthesis strategies have been developed to produce high-molecular-weight block copolymers with improved rheological performance and stability [23, 24].

The functionality of hydrophobically modified copolymer systems encompasses a broad spectrum of enhanced physicochemical properties and has been the focus of extensive research [25, 26]. In recent years, various associative copolymers have been developed, depending on the synthesis method, the type of interacting monomers, and the mode of hydrophobe incorporation - either as end groups (telechelic polymers) or as multiple small blocks distributed along the hydrophilic polymer backbone (multisticker polymers) [27, 28].

These hydrophobically modified polymer systems have been applied in cosmetics, drilling fluids, preparative chemistry, and as functional materials or coatings for food, textiles, and leather. However, their utilization in enhanced oil recovery (EOR) is relatively recent, and further optimization is required to design them effectively as chemical injection fluids for petroleum reservoirs [29, 30]. Feng et al. developed a hydrophobically modified polyacrylamide (HMA-PAM) incorporating 0.5% cetyl dimethylallyl ammonium chloride. The polymer demonstrated stability for up to 120 days at 45 °C; however, its performance at elevated reservoir temperatures was not evaluated. Given the lack of acrylamide units in the backbone, the polymer is anticipated to exhibit limited stability under more extreme thermal or saline conditions typically encountered in oil reservoirs [31]. Thermo-responsive hydrophobically associative water-soluble terpolymers have shown promise for enhanced oil recovery (EOR) of heavy crude oils in carbonate reservoirs. A terpolymer of acrylamide, N-isopropylacrylamide, and N,N′-dihexylacrylamide was synthesized via micellar free radical polymerization and characterized by NMR. Its rheological properties were evaluated across temperatures (25–120 °C) and salinities (1–5 wt% NaCl), and laboratory flooding tests with a heavy crude oil (2.26 Pa·s, 10.21° API) demonstrated significant improvements in oil recovery (68–75%), along with favorable adsorption and wetting behavior. These results indicate that such terpolymers can effectively enhance displacement efficiency under challenging reservoir conditions [32]. Poly-AM/AMPS microspheres were synthesized via aqueous polymerization to enhance deep sealing and profile control in low-permeability, heterogeneous reservoirs affected by water channeling. Their chemical structure was confirmed by FTIR, X-ray diffraction, and energy-dispersive spectroscopy, while thermal stability was evaluated through TG and DTG analyses. The microspheres exhibited a median particle size of 35.88 μm (range 1.94–497.8 μm) and a retention rate of 17.4% at 800 °C. Performance was further improved through functional modifications with maleic anhydride, sodium styrenesulfonate, dimethyl diallyl ammonium chloride, and nano-additives including SiO_2, graphene oxide, and S-$CaCO_3$. These modifications enhanced structural stability and thermal resistance, demonstrating the potential of Poly-AM/AMPS as an effective EOR agent in challenging reservoir conditions [33]. Ye et al. synthesized a hydrophobically associating copolymer via free-radical polymerization using acrylamide (AM), acrylic acid (AA), and N-allyloctadec-9-enamide (NAE) as monomers. Rheological tests demonstrated that the copolymer exhibited superior

viscosity and stability compared with partially hydrolyzed polyacrylamide. Moreover, an AM/AA/NAE/Tween-80 system effectively reduced interfacial tension and minimized surfactant loss due to stratum adsorption, highlighting its potential for enhanced oil recovery in polymer–surfactant flooding applications [34]. Previous studies have demonstrated that secondary waterflooding in carbonate reservoirs often results in limited oil recovery due to their inherent oil-wet nature and pronounced heterogeneity. To address these challenges, surfactant–polymer (SP) flooding has been developed by Ghosh as an effective enhanced oil recovery (EOR) method, combining interfacial tension (IFT) reduction, mobility control, and wettability alteration. Experimental investigations conducted at elevated reservoir conditions (80 °C and >90,000 ppm TDS) revealed that a carboxylate surfactant containing at least 30 ethylene oxide groups and a long hydrophobic tail provides superior tolerance to divalent cations. Coreflood experiments performed in Indiana limestone confirmed stable polymer transport without degradation and a significant improvement in oil displacement efficiency. The SP formulations achieved 77–92% recovery of residual oil, with low surfactant retention levels of 0.2–0.32 mg/g of rock, demonstrating that thermally stable and salt-tolerant chemical systems can substantially enhance oil recovery in high-temperature carbonate reservoirs [35].

Polymer flooding using hydrolyzed polyacrylamide (HPAM) enhances oil recovery by improving fluid mobility, though its effect on rock wettability remains debated. Molecular dynamics and experimental results showed that HPAM adsorption reduced the water contact angle to 130–140°, partially shifting the carbonate surface toward a water-wet state. While simulations indicated polymer desorption at higher temperatures, experiments revealed increased adsorption due to ion exchange and thermal effects. These findings highlight HPAM's dual role in viscosity control and wettability modification under reservoir conditions [36].

Chemical-assisted water injection has emerged as an effective method for enhancing heavy oil recovery by generating oil-in-water emulsions that markedly reduce crude viscosity.

In this context, novel star-like branched AM-SSS copolymers (SB-PAMs), synthesized via RAFT polymerization, demonstrated excellent potential for high-temperature polymer flooding. The synthesized polymers exhibited rapid solubility (0.75 h), high viscosity (45 mPa·s at 1000 mg/L and 50 °C), and strong emulsification capability, achieving up to 91.7% viscosity reduction and 90.4% dehydration efficiency.

Coreflooding results confirmed their superior EOR performance, with 800 mg/L SB-polymer yielding an additional 23.66% oil recovery after waterflooding and 19.46% improvement during hot-water flooding at 110 °C. These findings highlight the promise of SB-PAM copolymers as robust, thermally stable chemical agents for efficient heavy oil recovery under harsh reservoir conditions [18].

A novel thermothickening water-soluble polymer (PHAD) was synthesized to target high-temperature, high-salinity EOR. At a low concentration of only 0.2 wt% (total salinity 9350.08 mg/L), the PHAD polymer exhibited significant thermothickening ability. Upon increasing the temperature from 25 to 90 °C, its apparent viscosity increased up to 13.3 times.

Core displacement and etched glass microscopic model experiments confirmed its effectiveness in porous media, achieving a final oil recovery factor of 14.0 % compared to only 4.3 % for the homopolyacrylamide counterpart. These results confirm the PHAD copolymer is a highly suitable chemical for enhanced oil recovery under harsh reservoir conditions [37].

Building on these advancements, the present study focuses on the synthesis and comprehensive evaluation of a low cost high-molecular-weight terpolymer for enhanced oil recovery under challenging reservoir conditions. The work investigates polymer preparation, the polymer's rheological stability, viscoelastic behavior, and displacement efficiency in micromodel flooding experiments, considering the combined effects of temperature, salinity, injection rate, and polymer concentration.

By systematically characterizing the polymer's performance under controlled laboratory conditions, this research aims to address limitations observed in previous hydrophobically modified polymers and terpolymer systems, providing insights into the design of robust, thermally stable, and salinity-tolerant polymeric EOR agents for heterogeneous and high-temperature reservoirs.

2. Materials and Methods

2.1. Materials

The terpolymer was synthesized from three principal monomers: acrylamide (AM), maleic anhydride (MA), and styrene. Acrylamide (8 g) served as the main hydrophilic monomer, providing solubility and backbone flexibility according to (38-40).

Briefly, maleic anhydride (0.5 g) introduced anhydride functional groups to regulate block structure and improve salt tolerance, while styrene (1 g) acted as the hydrophobic monomer to enhance the polymer's thermal and mechanical stability. The aqueous phase was prepared using 20 mL of double-distilled deionized water. An inverse emulsion polymerization technique was employed.

Table 1. Physical and chemical properties of the initial materials used in terpolymer synthesis

Material	Chemical structure	Molecular weight (g/mol)	Density (g/cm³)	Purity (%)
Acrylamide (AM)	CH_2=CH–$CONH_2$	71.08	1.122	≥99
Maleic anhydride (MA)	$C_2H_2(CO)_2O$	98.06	1.480	—
Styrene	C_6H_5–CH=CH_2	104.15	0.909	≥99.9
Deionized water	H_2O	18.02	1.000	—
Cyclohexane	C_6H_{12}	84.16	0.778	≥99.9
Span 80	$C_{24}H_{44}O_6$ (approx.)	~428	~0.986	—
AIBN	$(CH_3)_2C(CN)N=N$ $C(CN)(CH_3)_2$	164.21	1.100	—

The continuous organic phase consisted of 100 mL of cyclohexane, selected for its hydrophobic characteristics. Span 80 (sorbitan monooleate, 1.5 g) was used as a nonionic surfactant to stabilize the water-in-oil emulsion.

Polymerization was initiated with α,α′-azoisobutyronitrile (AIBN, 0.006 g), an oil-soluble initiator that promoted free-radical generation within the organic phase.

All reagents were of analytical grade and used as received, except when further purification was required. The compositions of the initial reactants and their relevant physical and chemical properties are listed in Table 1.

2.2. Terpolymer Synthesis Methodology

The terpolymer was synthesized via a kind of inverse (water-in-oil) miniemulsion polymerization approach.

2.2.1. *Preparation of Phases*

The organic phase was prepared by dissolving 1.5 g of Span 80 in 100 mL of cyclohexane and homogenizing at 200 rpm. The aqueous phase consisted of 8 g acrylamide (AM) and 0.5 g maleic anhydride (MA) dissolved in 20 mL double-distilled water, which was degassed by boiling and nitrogen purging.

2.2.2. *Miniemulsion Formation and Initiation*

The aqueous phase was slowly injected into the organic phase over approximately 15 minutes using a syringe pump, while stirring was increased to 1800 rpm to form a stable miniemulsion. 1 g of purified styrene was then added dropwise.

The reactor temperature was gradually raised from 25 °C to 60 °C under continuous nitrogen flow. Polymerization was initiated by slowly injecting 0.006 g of AIBN dissolved in cyclohexane. The reaction proceeded for 4 hours at 60 °C with 2000 rpm stirring.

2.2.3. *Post-Polymerization Processing*

The resulting polymer latex was cooled and filtered using a Büchner funnel. It was washed multiple times with methanol to remove unreacted monomers and residual surfactant. The purified polymer was dried in an oven at 50–60 °C for 24 hours to yield a solid polymer powder.

2.3. Micromodel Fabrication and Characterization

2.3.1. *Design and Fabrication*

The porous micromodel structure was designed by analyzing CT scans of carbonate core samples using MATLAB to replicate reservoir heterogeneity. The design was fabricated onto an 8 mm thick glass plate using a precision laser etching system, ensuring vertical pore walls and accurate geometry.

Two glass plates were thermally bonded in a furnace by gradually heating to 670 °C over three hours and allowing natural cooling over three days, producing a stress-free, hermetically sealed structure. The design included interconnected channels and fracture-like regions (Fig. 1).

2.3.2. *Characterization*

Post-fabrication characterization revealed a porosity of approximately 58.97 %, an average pore radius of 14.16 µm (measured via capillary rise), and a total pore volume of 0.230 cm³.

2.3.3. *Injection Setup and Experimental Matrix*

Polymer solutions were injected using a high-precision laboratory syringe pump, as shown in Fig. 2. The experimental plan was designed to assess the terpolymer under the following controlled variables (Table 2). Injection rate for low, medium, and high rates (0.005–0.02 mL/min) to study front stability and sweep

efficiency. Salinity variation pre-flushing with seawater (SW), 2×SW, and 3×SW brine to evaluate the effect of ionic strength. Temperature variation experiments were conducted at 25 °C, 50 °C, and 80 °C using a temperature-controlled bath.

2.4. Characterization

Post-fabrication analysis verified the micromodel structure, revealing a porosity of approximately 58.97 %, an average pore radius of 14.16 µm (determined via capillary rise), and a total pore volume of 0.230 cm³.

2.6. Polymer Solution Preparation

Polymer solutions were prepared at 500 ppm, 750 ppm, and 1000 ppm for micromodel experiments. The solutions were thoroughly degassed using either gentle nitrogen purging or mild vacuum to remove entrapped air and prevent interference during injection.

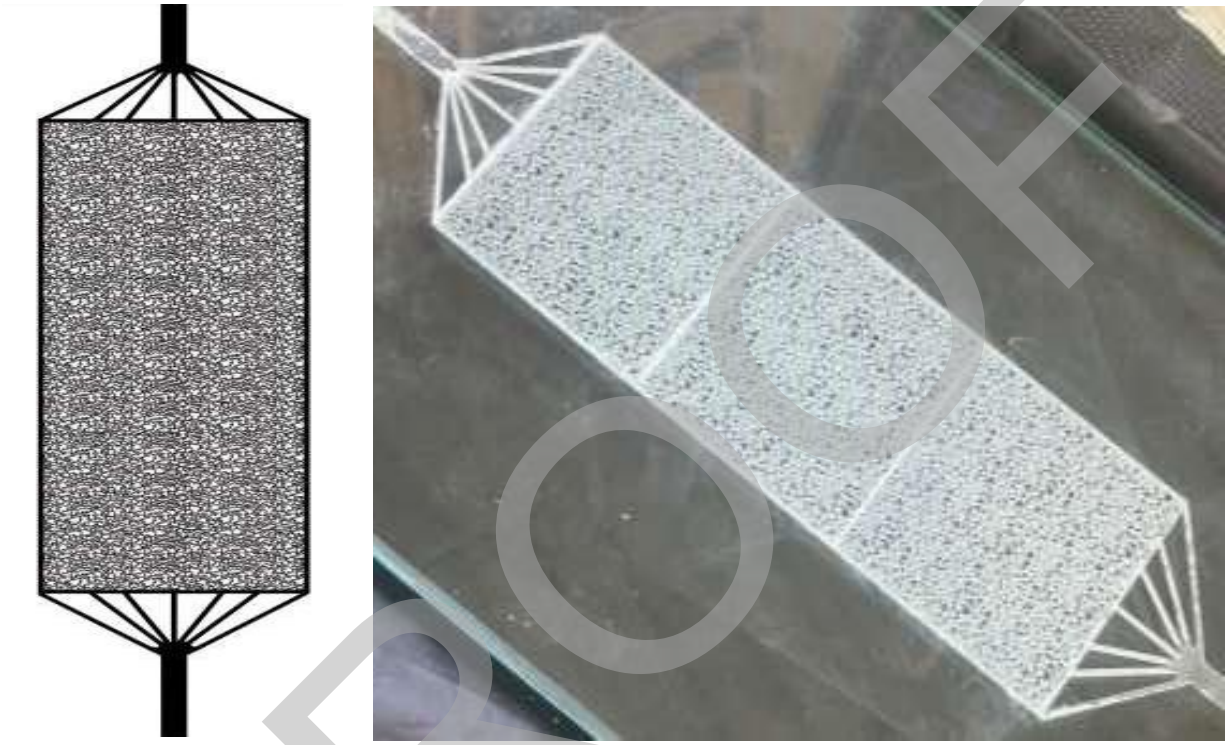

Figure 1. Two micromodel designs: (a) single-block micromodel, and (b) three-block micromodel etched on glass

Table 2. Detailed experimental matrix for micromodel injection tests

Test Group	Polymer Concentrations (ppm)	Variable Parameter	Parameter Levels	Purpose
Rate Variation Test	500, 750, 1000	Injection rate	Low (e.g., 0.005 mL/min) Medium (e.g., 0.01 mL/min) High (e.g., 0.02 mL/min)	Investigate influence of injection velocity on front stability and sweep efficiency.
Salinity Variation Test	500, 750, 1000	Salinity	SW (seawater salinity) 2× SW 3× SW	Assess polymer performance in various ionic strengths representative of reservoir brines.
Temperature Variation Test	500, 750, 1000	Temperature	25 °C 50 °C 80 °C	Evaluate thermal stability and viscosity retention of polymer solutions at different reservoir-like temperatures.

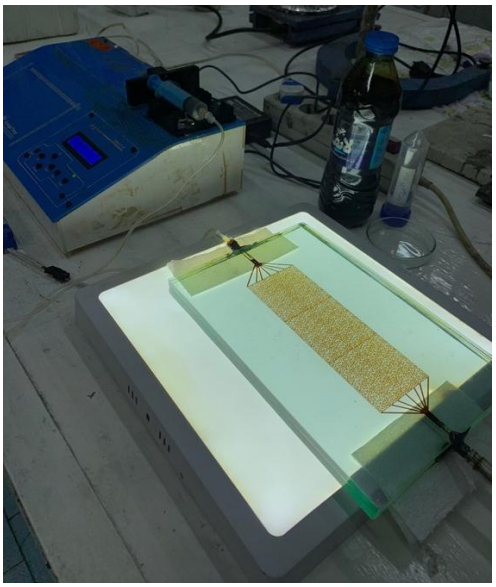

Figure 2. Setup of the micromodel system

2.7. Analytical and Characterization Methods

The synthesized terpolymer was characterized using multiple analytical techniques at the laboratory facilities of Sharif University of Technology to confirm its chemical structure, molecular properties, and rheological behavior: FT-IR Spectroscopy was conducted on a Bruker Tensor 27 spectrometer over the range 4000-600 cm^{-1} using the KBr pellet method to verify functional groups and overall chemical structure. ^1H NMR spectroscopy was performed on a Bruker AVANCE III 400 MHz spectrometer using deuterium oxide (D_2O) as solvent to confirm the formation of the terpolymer and structural integrity. X-ray Diffraction (XRD) was carried out on a PANalytical X'Pert PRO diffractometer (Cu Kα) to examine crystalline or amorphous structural characteristics.

Field Emission Scanning Electron Microscopy (FE-SEM) Observations were made on gold-coated samples using a TESCAN MIRA3 FE-SEM to assess surface morphology and particle size. Dynamic Light Scattering (DLS) was conducted using a Malvern Zetasizer Nano ZS to evaluate particle size distribution and microstructural characteristics. Capillary viscometry measurements were performed with an Ubbelohde viscometer at 25 °C to determine intrinsic viscosity [η] and estimate the viscosity-average molecular weight (Mv) via the Mark-Houwink equation.

Gel Permeation Chromatography (GPC) was carried out on a Waters Alliance GPC system to obtain accurate molecular weight parameters (Mw, Mn) and the polydispersity index (PDI).

Rheological Measurements were performed with an Anton Paar rotational rheometer under steady shear to study the effects of polymer concentration, temperature (30 °C, 50 °C, 80 °C), and varying salinity on solution viscosity.

3. Results and Discussion

Intrinsic viscosity and viscosity average molecular weight of the synthesized terpolymer were determined through capillary viscometry using an Ubbelohde glass viscometer at 25 °C in dilute aqueous solution. The rheological behavior observed for the terpolymer solutions is characteristic of hydrophobically modified water-soluble polymers. The reduced viscosity (η_{red}) shows a sharp, nonlinear increase at a certain critical concentration. This sudden rise signifies a crucial transition: at low concentrations, (η_{red}) exhibits a nearly linear, dilute-solution behavior dominated by intramolecular hydrophobic interactions (within a single chain). Beyond the critical concentration, these interactions shift to significant intermolecular associations (between different chains). This intermolecular association leads to enhanced chain entanglement and reduced chain mobility, which manifests as the substantial rise in the overall solution viscosity. The relationship between the specific viscosity (η_{sp}) and polymer concentration further highlights this concentration-dependent rheological behavior. The intrinsic viscosity [η] a measure of the polymer's individual hydrodynamic volume, was calculated by applying the Huggins equation and linearly extrapolating the reduced viscosity data to zero concentration. This intrinsic viscosity was then used to estimate the viscosity-average molecular weight (M_v) of the terpolymer via the Mark–Houwink equation $[\eta] = 6.31 \times 10^{-3} M_v^{0.8}$, utilizing parameters established for polyacrylamide systems. It is important to note that while this approach provides a reliable estimate, the calculated (M_v) is considered an approximation. This is because the Mark–Houwink constants, derived for linear polyacrylamide, do not fully account for the strong intermolecular associations driven by the hydrophobic styrene segments in the terpolymer. Nonetheless, the viscometric analysis confirms the terpolymer possesses a high intrinsic viscosity and significant molecular weight, properties that are essential for successful enhanced oil recovery (EOR) applications where solution viscosity and effective chain entanglement are key performance factors. Additionally, Gel Permeation Chromatography GPC was conducted to confirm the molecular weight and distribution of the synthesized terpolymer, providing a more precise measurement to validate the earlier viscometer estimate. The resulting molecular weight distribution curve shows a relatively broad distribution, which is typical for synthetic polymers created via free-radical polymerization.

Table 3. The intrinsic viscosity and molecular weight data

Method	Intrinsic viscosity (dl/g)	Average molecular weight × 10^{-6} (g/mol)
$[\eta]=Lim_{C\to 0}\left(\frac{\eta_{sp}}{C}\right)$	12.11	4.01
$[\eta]=Lim_{C\to 0}\left(\frac{\partial \ln \eta_{rel}}{\partial C}\right)$	11.97	3.95

The GPC analysis yielded a weight-average molecular weight Mw of approximately 10.6 × 10^6 g/mol and a number-average molecular weight Mn of approximately 4.37 × 10^6 g/mol. This data results in a dispersity Đ, calculated as Đ = M_w / M_n, of 2.44. This Đ indicates a moderate degree of dispersity, consistent with a high-molecular-weight polymer designed for demanding applications. The GPC results confirm the successful synthesis of a high-molecular-weight terpolymer. The molecular weight values obtained from GPC are generally higher than those estimated by viscometry, a difference commonly explained by the distinct measurement principles: GPC directly separates and assesses the molecular size distribution, while viscometric methods rely on correlations with hydrodynamic volume. The high Mw and controlled, broad distribution supports the terpolymer's suitability for EOR applications requiring efficient mobility control and strong viscosifying performance. The intrinsic viscosity and molecular weight data are compared in Table 3. The intrinsic viscosity [η], measured via capillary viscometry and extrapolated using the Huggins equation, shows a value of 12.11 (or dl/g (11.97 dL/g if the second row represents a confirmation run). The corresponding viscosity-average molecular weight Mv, calculated using the Mark–Houwink equation, is 4.01 × 10^6g/mol. These viscometric results are contrasted with the GPC analysis, which yields the weight-average molecular weight Mw. This high intrinsic viscosity and significant molecular weight, as quantitatively compared in Table 3, confirm the synthesized terpolymer's ability to form large, effective hydrodynamic coils in solution, which is the physical basis for its high viscosifying power essential for effective mobility control in enhanced oil recovery EOR applications. Rheological measurements were conducted using a rotational rheometer at controlled shear rates and temperatures, with the results visually presented in Fig. 3.

Shear-Thinning Behavior

As shown in Fig. 3 (top left, top right, and bottom left), the terpolymer solutions at all tested concentrations and temperatures (30, 50, and 80 °C) consistently exhibit shear-thinning behavior. That is, the viscosity of the solution decreases sharply as the shear rate increases. This non-Newtonian behavior is characteristic of high-molecular-weight polymer solutions where the coiled chains align themselves with the flow field at higher shear rates, reducing hydrodynamic resistance and facilitating mobility control in porous media.

Effect of Concentration (Viscosity vs. Concentration)

At any given temperature and shear rate, the solution viscosity consistently increases with increasing polymer concentration (from 500 to 1000 ppm). This is attributed to enhanced chain entanglement and intermolecular interactions. As the polymer chains become denser, the likelihood of physical overlap and interaction increases significantly, leading to a substantial enhancement in viscosity, a mechanism vital for improving the sweep efficiency of the injected fluid.

Effect of Temperature (Viscosity vs. Temperature)

The results demonstrate the polymer's excellent thermal stability, showing the solution viscosity actually increases with increasing temperature (e.g., comparing 30 to 80 °C at a constant shear rate). This phenomenon, often unique to certain associative polymers, is explained by the improved solubility and hydration of the polymer chains at elevated temperatures. Increased thermal energy facilitates better polymer chain expansion and dispersion, causing the chains to adopt a more extended conformation in the solvent, which effectively results in a higher hydrodynamic volume and consequently a higher solution viscosity.

Zero-Shear Viscosity

Fig. 3 (bottom right) summarizes the zero-shear viscosity values, which represent the solution's viscosity under near-static conditions. This plot clearly illustrates a strong synergistic effect where the highest viscosities are achieved at the highest concentration (1000 ppm) and the highest temperature (80 °C).

This finding confirms the terpolymer's ability to maintain and even enhance its thickening power under elevated reservoir conditions, solidifying its status as a promising candidate for EOR applications where both high viscosity and temperature stability are paramount for effective sweep and mobility control.

To fully characterize the polymer's performance in simulated reservoir environments, the viscoelastic behavior, including complex viscosity (η*) and storage modulus (G'), was measured during a temperature sweep from 30 °C to 80 °C in the presence of NaCl.

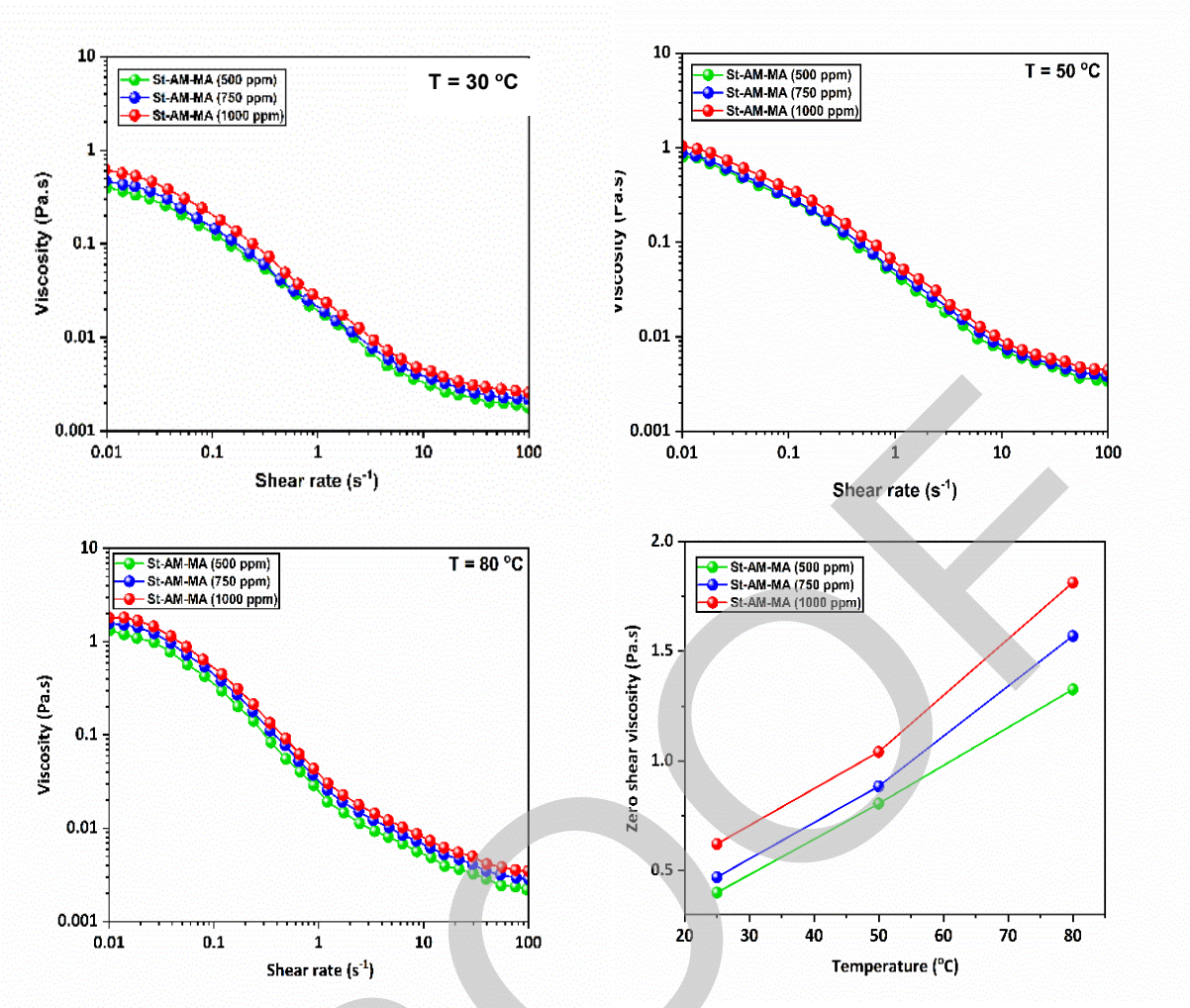

Figure 3. Effect of terpolymer concentration and temperature on the viscosity of aqueous solutions

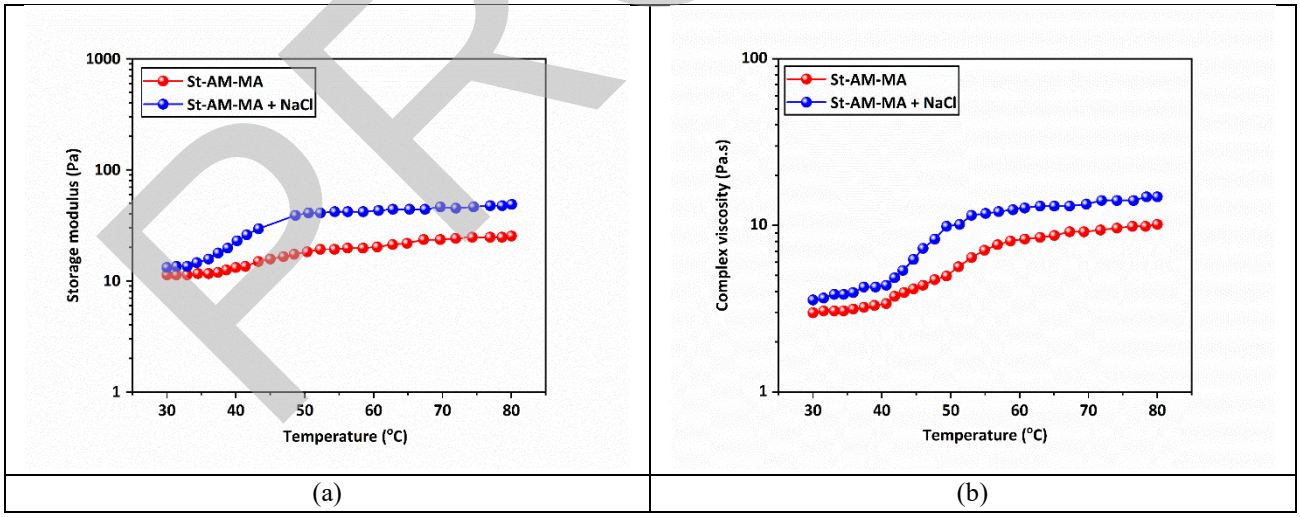

Figure 4. Temperature-dependent changes in (a) complex viscosity and (b) storage modulus of the terpolymer solution in the presence of NaCl

The results are presented in Fig. 4, showing both η* (Fig. 4(a)) and G' (Fig. 4(b)) The temperature-dependent trends in both complex viscosity and storage modulus can be systematically divided into three stages. In the first stage, ranging from 30 °C to approximately 40 °C, only a slight change in both η* and G' is observed. This indicates that at lower temperatures, the thermal energy has a minimal impact on the existing chain mobility and the initial structural network of the polymer solution. The second stage, spanning between 40 °C and approximately 50 °C, is characterized by a more pronounced increase in both the complex viscosity and

the storage modulus. This notable behavior is due to rising temperature leading to improved solvation and expansion of the polymer chains. Crucially, the presence of NaCl likely facilitates this process by screening the electrostatic repulsions between polymer segments, thereby promoting closer chain interactions. This enhanced association leads to the formation of a partial polymer network, signified by the jump in the storage modulus (G'), which reflects the development of the solution's elastic or solid-like character. In the third stage, extending from 50 °C to 80 °C, a moderate yet continuous increase in both η* and G' is maintained. This sustained upward trend confirms the further stabilization and reinforcement of the polymer network structure at higher temperatures, despite the increased molecular motion. This temperature-dependent enhancement of viscosity and modulus in saline conditions is highly desirable for EOR applications. The ability of the solution to maintain or increase its viscoelastic properties in high-temperature, high-salinity reservoir environments ensures better mobility control, improved sweep efficiency, and ultimately higher oil recovery factors. The synthesized terpolymer thus demonstrates excellent thermal stability and favorable viscoelastic properties, supporting its potential for practical application in challenging EOR scenarios.

Oil Recovery Performance in Micromodel Tests

Micromodel Flooding Tests

To evaluate the displacement efficiency and flow behavior of the synthesized terpolymer under controlled conditions, a systematic series of micromodel flooding experiments was designed. These tests utilize a transparent, etched-glass model which allows for the direct visualization of fluid displacement at the pore scale. This setup provides crucial insights into microscopic flow mechanisms, specifically fingering, channeling, and sweep efficiency, which govern oil recovery during polymer flooding. The study systematically investigates the influence of three critical operational parameters to assess the polymer's adaptability to varying reservoir conditions. (1) The terpolymer solution was tested at three distinct concentrations: 500 ppm, 750 ppm, and 1000 ppm. By varying the concentration, the direct impact of viscosity and mobility control on oil displacement performance can be assessed. (2) Tests were conducted at 30 °C, and 80 °C. This range covers typical to high reservoir temperatures, providing insight into the polymer solution's thermal stability and adaptability. (3) The influence of ionic strength was explored using three salinity levels: seawater salinity (SW), two times seawater salinity (2times SW), and three times seawater salinity (3times SW). This approach is essential for assessing the polymer's tolerance to high ionic strength and its efficiency in high-salinity field environments. this systematic micromodel study provides a comprehensive, visual evaluation of the terpolymer's performance across a range of operational parameters, supporting its potential application in enhanced oil recovery.

Effect of Injection Rate on Oil Recovery Performance

The injection rate of the displacing fluid plays a critical role in determining the stability of the displacement front and the extent of viscous fingering during flooding operations. In porous media, a high injection rate typically intensifies interfacial instabilities, especially when the displacing phase (e.g., polymer solution or water) exhibits a lower viscosity than the resident oil. This imbalance often results in premature breakthrough and poor volumetric sweep efficiency. The experimental results presented in Tables 4 and 5 clearly demonstrate this phenomenon. At a rapid injection rate corresponding to a total injection time of 1 hour, the remaining oil saturation remained relatively high. Specifically, the oil saturation decreased only marginally from 64.27% after waterflooding to 63.95% following polymer flooding, indicating minimal incremental oil displacement. The total oil recovery factor at this rate was 36.05%, confirming the limited efficiency of rapid injection. Visual observation of the micromodel further revealed pronounced viscous fingering patterns, with elongated flow channels bypassing substantial oil volumes in lower-permeability regions. This uneven flow behavior reflects the inability of the polymer solution to uniformly penetrate the pore network under high flow conditions. When the injection duration was increased to 3 and 5 hours, the oil displacement efficiency improved considerably. The remaining oil saturation decreased to 57.23% and 56.71%, respectively, signifying enhanced sweep and displacement of previously bypassed oil zones. Correspondingly, the overall recovery factor rose from 36.05% at the fastest rate to 42.77% and 43.29% at longer injection durations. These results indicate that lower injection rates effectively suppress viscous fingering, allowing the polymer solution to establish a more stable displacement front and achieve deeper penetration into the porous matrix. The improved sweep at reduced flow rates suggests that the mobility ratio between oil and the displacing fluid was better controlled, leading to more uniform displacement and reduced channeling. Nevertheless, this improvement in recovery efficiency must be balanced against operational and economic considerations.

Table 4. Effect of Injection Rate

Injection Time	Initial Oil Saturation (%)	Oil Saturation After Waterflood (%)	Final Oil Saturation (%)
1 hour	100	64.27	63.95
3 hours	100	60.86	57.23
5 hours	100	58.76	56.71

Table 5. Recovery Rate at Different Injection Durations

Injection Time	Recovery Factor (%)
1 hour	36.05
3 hours	42.77
5 hours	43.29

While slower injection enhances the quality of displacement and increases ultimate recovery, it simultaneously reduces volumetric throughput and may extend production times in field-scale operations. Thus, the practical implementation of low injection rates requires a comprehensive techno-economic evaluation to determine whether the gain in recovery efficiency compensates for the reduction in production rate. Optimization of injection parameters should therefore aim to achieve an optimal balance between recovery enhancement and economic feasibility, ensuring sustainable and efficient polymer flooding performance in heterogeneous reservoirs.

Effect of Polymer Concentration

Polymer concentration plays a crucial role in determining the effectiveness of oil displacement during flooding operations, as it directly influences the viscosity of the injected fluid and the resulting mobility ratio between the displacing and displaced phases. The micromodel experiments clearly demonstrated that variations in polymer concentration strongly affected the recovery performance and sweep uniformity (Tables 6 and 7).

At the lowest polymer concentration of 500 ppm, the flooding process exhibited negligible improvement compared to conventional waterflooding. The total oil recovery plateaued at approximately 64% of the original oil in place (OOIP), remaining almost unchanged before and after polymer injection.

The incremental oil recovery was limited to only ~0.3% of OOIP, indicating that this concentration was insufficient to produce any significant viscosity enhancement or mobility control. The displacement front remained unstable, characterized by pronounced viscous fingering similar to that observed in waterflooding.

Visual inspection of the micromodel confirmed that large regions of oil remained trapped in low-permeability channels and dead-end pores, reflecting the poor sweep efficiency associated with low polymer concentration.

A marked improvement in displacement behavior was observed at 750 ppm, where polymer flooding achieved a noticeable increase in oil recovery. The final oil saturation decreased from 62.37% (after waterflooding) to 59.6%, corresponding to an incremental recovery of approximately 2.8% of OOIP.

Although the improvement was moderate, it demonstrated enhanced mobility control, with the higher-viscosity polymer solution propagating more uniformly through the micromodel.

The visual observations supported this trend, showing fewer trapped oil pockets and a more stable displacement front compared with the 500 ppm case. The reduction in viscous fingering at this concentration indicates improved sweep efficiency and more effective displacement of bypassed oil zones.

The most significant enhancement was achieved at the highest polymer concentration of 1000 ppm. In this case, the total oil recovery increased from 54.9% after waterflooding to 62.2% of OOIP, yielding an incremental recovery of approximately 7.3% of OOIP the largest observed improvement.

The high remaining oil saturation after waterflooding (~45% of OOIP) provided considerable potential for enhanced recovery. The viscous polymer solution at this concentration effectively mobilized a substantial portion of the residual oil, resulting in a nearly complete sweep of the micromodel. Final images revealed a uniform displacement front with minimal fingering and only a few isolated residual oil clusters.

Overall, the data clearly indicate that increasing polymer concentration significantly enhances displacement efficiency and recovery performance. As shown in Table, the recovery factor improved progressively from 36.05% at 500 ppm to 40.4% at 750 ppm, and further to 45.09% at 1500 ppm.

This consistent trend highlights the direct correlation between polymer concentration, solution viscosity, and mobility control. Higher polymer concentrations enhance the viscous force balance at the flood front, suppressing fingering instabilities and promoting a more uniform sweep through the porous network.

However, polymer concentration must be carefully optimized in EOR applications to achieve maximum recovery while maintaining injectivity and economic feasibility.

Table 6. Oil Saturation after Flooding vs Polymer Concentration

Polymer Concentration (ppm)	Initial Oil Saturation (%)	Oil Saturation After Waterflood (%)	Final Oil Saturation (%)
500	100	64.27	63.95
750	100	62.37	59.6
1500	100	62.15	54.91

Table 7. Recovery Factor vs Polymer Concentration

Polymer Concentration (ppm)	Recovery Factor (%)
500	36.05
750	40.4
1500	45.09

It is noteworthy that although the absolute final recovery values (around 62–64% OOIP) did not vary monotonically with concentration partly due to minor variations in initial waterflood performance the incremental recovery attributable to polymer injection clearly increased with polymer concentration. The 500 ppm flood yielded a recovery factor of 36.05% (essentially identical to waterflooding), while 750 ppm and 1000 ppm floods increased the recovery to approximately 40.4% and 45.09%, respectively. This progressive improvement indicates that higher polymer concentrations enhanced sweep efficiency and reduced the amount of residual oil. The combined evidence from both the production data and micromodel imaging thus confirms that increasing polymer concentration effectively improves mobility control, stabilizes the displacement front, and leads to a more uniform and efficient recovery of oil in porous media.

Effect of Temperature

Temperature exhibited a strongly adverse influence on polymer flooding efficiency, primarily due to its impact on polymer viscosity and stability. As temperature increased, the polymer solution lost its thickening ability, reducing its capacity to improve the mobility ratio and displace trapped oil effectively.

At 30 °C, the polymer flood achieved a noticeable enhancement in oil recovery relative to waterflooding. Under these ambient conditions, the oil recovery after waterflooding was approximately 65.4% OOIP, which increased to 67.1% OOIP following polymer injection, an incremental gain of about 1.7% OOIP. Although this improvement was modest, it clearly reflected the beneficial role of viscosity-induced mobility control at low temperatures. The flood front was relatively stable, and the polymer solution with its highest viscosity at 30 °C was able to more uniformly sweep the micromodel. Visual observations confirmed this effect: the displacement appeared homogeneous, with the polymer accessing previously unswept pores and leaving behind only small, isolated oil clusters. These results indicate efficient oil recovery at 30 °C due to favorable rheological behavior of the polymer solution.

At 50 °C, however, polymer flooding performance deteriorated markedly. The reduction in polymer viscosity at elevated temperature consistent with the rheological data led to a poorer mobility ratio and reduced sweep efficiency. Under these conditions, the polymer flood recovered almost no additional oil, with total recovery rising only slightly from 63.95% to 64.27% OOIP, representing a marginal incremental recovery of ~0.3% OOIP. In essence, the polymer behaved similarly to water, resulting in early breakthrough and limited displacement. The visual patterns in the micromodel supported this observation: extensive channeling through high-permeability pathways and large oil-filled regions persisted even after polymer injection. The diminished performance at 50 °C is attributed to viscosity loss and potential polymer adsorption or partial thermal degradation, both of which hinder the solution's ability to control flow in porous media. Further increasing the temperature to 80 °C effectively nullified the enhanced oil recovery (EOR) effect of the polymer. The total recovery changed minimally from 64.25% after waterflooding to 64.59% OOIP after polymer flooding again yielding an incremental gain of only ~0.3% OOIP. The polymer solution at this temperature likely experienced significant viscosity loss, approaching that of water, and possibly underwent thermal degradation that further compromised its rheological properties. Consequently, the injected fluid behaved nearly as a simple waterflood, producing extensive viscous fingering and leaving substantial volumes of oil unswept. The negligible improvement observed at 80 °C may fall within the experimental uncertainty range, underscoring that the polymer had effectively lost its EOR functionality at this high temperature. Overall, the micromodel experiments clearly illustrate that polymer flooding efficiency declines sharply with increasing temperature. As summarized in Tables 8 and 9, the polymer at 30 °C yielded the highest incremental recovery (~1.7% OOIP), while at 50 °C and 80 °C the improvement was practically negligible. This decline in recovery is directly correlated with the temperature sensitivity of polymer viscosity. As the polymer becomes less viscous and potentially unstable at higher temperatures, it fails to maintain an optimal mobility ratio or access residual oil in low-permeability zones.

Table 8. Oil Saturation vs Temperature

Temperature (°C)	Initial Oil Saturation (%)	Oil Saturation After Waterflood (%)	Final Oil Saturation (%)
25	100	64.27	63.95
50	100	67.1	65.37
80	100	64.59	64.25

Table 9. Recovery Rate vs Temperature

Temperature (°C)	Recovery Factor (%)
25	36.05
50	34.63
80	35.73

Therefore, unless thermally stable polymers or higher concentrations are employed, conventional polymer flooding provides diminishing or negligible benefits under elevated temperature conditions, as clearly demonstrated by these micromodel results.

Effect of Salinity

Salinity exerted a significant influence on polymer flooding performance, primarily by reducing the viscosity and thickening ability of the polymer solution, thereby diminishing its capacity to enhance sweep efficiency.

The experiments were designed to isolate salinity as the sole variable all tests were conducted at constant polymer concentration and ambient temperature. Three salinity levels were evaluated: base seawater (~35,000 ppm TDS), twice seawater (2× SW), and three times seawater (3× SW). The results consistently demonstrated that increasing salinity adversely affected the polymer's ability to improve oil recovery in the micromodel experiments.

Under seawater conditions, polymer flooding led to a noticeable enhancement in oil recovery beyond waterflooding. After the waterflood stage, approximately 56.7% OOIP had been recovered, leaving about 43.3% of the oil in place. Subsequent polymer injection mobilized several additional percent of OOIP, resulting in the highest incremental gain among the salinity levels tested. While the precise final recovery value for the seawater case was partially obscured in the data, the qualitative and visual evidence confirmed that seawater polymer flooding produced the most effective sweep, yielding approximately 3–5% OOIP additional recovery.

The micromodel image supports this observation, showing that the polymer successfully penetrated oil-rich zones left unswept by waterflooding, thereby creating a cleaner and more uniform displacement pattern. Some residual oil droplets persisted in small pore throats, but overall, the seawater polymer flood demonstrated the best recovery efficiency.

At 2× seawater salinity, polymer performance declined drastically. During this test, waterflooding alone recovered 61.4% OOIP, leaving 38.6% oil in place. However, polymer flooding under this high-salinity condition produced almost no incremental recovery the total recovery increased only to 62.2% OOIP, representing a negligible 0.8% OOIP gain. The polymer's behavior was nearly identical to that of plain water, suggesting severe viscosity loss caused by ionic screening and polymer coil contraction.

The visual displacement pattern confirmed this: the injected solution followed dominant high-permeability channels while bypassing large volumes of oil in tighter regions. Such poor sweep efficiency is consistent with the known physicochemical effects of salinity on HPAM-type polymers, where high ionic strength compresses the polymer's electrical double layer and reduces molecular expansion, leading to a lower viscosity and poorer mobility ratio.

Interestingly, at 3× seawater salinity, polymer flood performance while still poor showed a slight improvement over the 2× case. Here, the waterflood recovered 60.7% OOIP, and polymer injection raised the total recovery to 63.7% OOIP, corresponding to an incremental recovery of approximately 2.9% OOIP. Although this increase was modest, it indicates that some additional oil was displaced, possibly due to experimental variability or minor flow diversion effects caused by polymer aggregation or localized plugging in high-salinity brine.

The micromodel photograph (Fig. 4) revealed that the displacement front remained unstable and finger-like, though small previously unswept oil pockets were mobilized more effectively than in the 2× case. Nonetheless, the overall recovery remained significantly lower than in the seawater condition, reinforcing that high salinity greatly compromises polymer flood efficiency.

As summarized in Tables 10 and 11, polymer flooding effectiveness decreased systematically with increasing salinity. At 2× SW, total recovery increased only from 61.38% to 62.22%, while at 3× SW, the increase was slightly higher, from 60.71% to 63.65%. In contrast, the seawater case (SW) achieved a substantial improvement, with recovery rising from 56.72% after waterflooding to 61.02% after polymer flooding, corresponding to a 43.28% recovery factor the highest among all cases.

Table 10. Oil Saturation vs Salinity

Salinity Condition	Initial Oil Saturation (%)	Oil Saturation After Waterflood (%)	Final Oil Saturation (%)
SW	100	61.02	56.72
2× SW	100	62.22	61.38
3× SW	100	63.65	60.71

Table 11. Recovery Rate Vs Salinity

Salinity Condition	Recovery Factor (%)
SW	43.28
2× SW	38.62
3× SW	39.29

This decline in performance with salinity directly correlates with the rheological behavior of the polymer solution: higher ionic strength compresses polymer coils and reduces chain extension, leading to a sharp drop in viscosity and, consequently, poorer mobility control.

In summary, the micromodel results conclusively demonstrate that polymer flooding efficiency decreases with increasing brine salinity. The polymer's reduced viscosity at elevated ionic strength prevented stable flood-front propagation and resulted in extensive viscous fingering, early breakthrough, and large unswept zones. Thus, in high-salinity environments, standard HPAM-based polymers lose much of their EOR capability. To achieve meaningful oil recovery under such conditions, polymer formulations must be optimized either by increasing polymer concentration, adding salt-tolerant co-monomers, or using specially designed associative or hydrophobically modified polymers to restore viscosity and maintain effective mobility control.

3. Conclusions

A hydrophobically associative terpolymer with low cost monomers and one step process was successfully synthesized and comprehensively characterized for EOR purposes. TGA/DTG results established good thermal stability. Rheological evaluation revealed excellent shear-thinning behavior and significant viscosity retention at moderate temperature and high salinity, indicative of stable hydrophobic associations.

The micromodel flooding experiments conducted in this study highlight the acrylamide- styrene maleic anhydride terpolymer's efficacy as a robust EOR agent for heterogeneous carbonate reservoirs, where porosity of approximately 58.97%, pore radii averaging 14.16 µm, and interconnected channels with fracture-like regions mimic real-world heterogeneity. Across polymer concentrations of 500–1000 ppm, the terpolymer exhibited sustained rheological stability and viscoelastic properties under injection rates of 0.005–0.02 mL/min, demonstrating improved front stability and sweep efficiency compared to baseline waterflooding. Salinity variations from seawater to 3×SW brines confirmed tolerance to elevated ionic strengths representative of reservoir fluids, with minimal degradation in displacement performance. Temperature tests at 25–80°C further validated exceptional thermal stability, retaining viscosity and promoting uniform oil mobilization without significant channeling. These findings underscore the terpolymer's potential to overcome key challenges in high-temperature, high-salinity environments, offering insights for optimizing polymer flooding designs in heterogeneous reservoirs to achieve higher residual oil recovery factors.

Authors Contribution
All the authors have participated sufficiently in the intellectual content, conception and design of this work or the analysis and interpretation of the data (when applicable), as well as the writing of the manuscript.

Availability of data and materials
The data that support the findings of this study are available from the corresponding author, upon reasonable request.

Conflict of interests
The author states that there is no conflict of interest.

References

[1] Gbadamosi A, Patil S, Kamal MS, Adewunmi AA, Yusuff AS, Agi A, et al. Application of polymers for chemical enhanced oil recovery: a review. Polymers. 2022;14(7):1433. https://doi.org/10.3390/polym14071433

[2] Xiangguo L, Bao C, Kun X, Weijia C, Yigang L, Xiaoyan W. Enhanced oil recovery mechanisms of polymer flooding in a heterogeneous oil reservoir. Petroleum Exploration and Development. 2021;48(1):169-178. https://doi.org/10.1080/10916466.2024.2442506

[3] Marquez R, Ding H, Barrios N, Vera RE, Salager J-L, Al-Shalabi EW, et al. Recent Advances in Enhanced Oil Recovery with Low-Salinity Waterflooding and Its Hybrid Methods in Carbonate Reservoirs. Energy & Fuels. 2025;39(19):8769-8799. https://doi.org/10.1021/acs.energyfuels.4c06023

[4] Zeynalli M, Mushtaq M, Al-Shalabi EW, Alfazazi U, Hassan AM, AlAmeri W. A comprehensive review of viscoelastic polymer flooding in sandstone and carbonate rocks. Scientific Reports. 2023;13(1):17679. https://doi.org/10.1038/s41598-023-44896-9

[5] Hassan AM, Al-Shalabi EW, Ayoub MA. Updated perceptions on polymer-based enhanced oil recovery toward high-temperature high-salinity tolerance for successful field applications in carbonate reservoirs. Polymers. 2022;14(10):2001. https://doi.org/10.3390/polym14102001

[6] Khlaifat AL, Fakher S, Harrison GH. Evaluating factors impacting polymer flooding in hydrocarbon reservoirs: laboratory and field-scale applications. Polymers. 2023;16(1):75. https://doi.org/10.3390/polym16010075

[7] Adel IA, Hassan AM, Al-Shalabi EW, AlAmeri W, editors. A look ahead to the future of surfactant flooding EOR in carbonate reservoirs under harsh conditions of high temperature and high salinity. SPE Gas & Oil Technology Showcase and Conference; 2023: SPE. https://doi.org/10.2118/214154-MS

[8] Bhut PR, Pal N, Mandal A. Characterization of hydrophobically modified polyacrylamide in mixed polymer-gemini surfactant systems for enhanced oil recovery application. ACS omega. 2019;4(23):20164-20177. http://doi.org/10.1021/acsomega.9b02279

[9] Khan M. Chemical and physical architecture of macromolecular gels for fracturing fluid applications in the oil and gas industry; current status, challenges, and prospects. Gels. 2024;10(5):338. https://doi.org/10.3390/gels10050338

[10] Liu Z, Feng Q, Xu Z, Yang S. Research Progress of Molecular Simulation in Acrylamide Polymers with High Degree of Polymerization. Molecules. 2024;29(11):2589. https://doi.org/10.3390/molecules29112589

[11] Yang J, Wang J, Zhang J, Du X, Liu Q, Zhang H. Research progress of polyacrylamide polymerization in fracturing: a mini review. Petroleum Science and Technology. 2024:1-13. https://doi.org/10.1080/10916466.2024.2442506

[12] Wu G, Yu L, Jiang X. Synthesis and properties of an acrylamide-based polymer for enhanced oil recovery: A preliminary study. Advances in Polymer Technology. 2018;37(8):2763-2773. https://doi.org/10.1002/adv.21949

[13] Cao J, Song T, Zhu Y, Wang S, Wang X, Lv F, et al. Application of amino-functionalized nanosilica in improving the thermal stability of acrylamide-based polymer for enhanced oil recovery. Energy & fuels. 2018;32(1):246-254. https://doi.org/10.1021/acs.energyfuels.7b03053

[14] Duan S, Hua M, Zhang CW, Hong W, Yan Y, Jazzar A, et al. Noncovalent Aggregation for Diverse Properties in Hydrogels: A Comprehensive Review. Chemical Reviews. 2025. https://doi.org/10.1021/acs.chemrev.5c00069

[15] Shi S, Sun J, Lv K, Liu J, Bai Y, Wang J, et al. Fracturing fluid polymer thickener with superior temperature, salt and shear resistance properties from the synergistic effect of double-tail hydrophobic monomer and nonionic polymerizable surfactant. Molecules. 2023;28(13):5104. https://doi.org/10.3390/molecules28135104

[16] Wu R, Yan Y, Li X, Tan Y. Preparation and controllable heavy oil viscosity reduction performance of pH-responsive star block copolymers. Journal of Molecular Liquids. 2023;389:122925. https://doi.org/10.1016/j.molliq.2023.122925

[17] Han C, Li R, Lu Y. Study on synthesized thermoresponsive block copolymer for water-based oil sands extraction. Energy & Fuels. 2020;34(8):9473-9482. https://doi.org/10.1021/acs.energyfuels.0c01585

[18] Zhao C, Zhang J, Lv J, Huang B, Yang G, Tang E, et al. Development of Novel Star-Like Branched-Chain Acrylamide (AM)-Sodium Styrene Sulfonate (SSS) Copolymers for Heavy Oil Emulsion Viscosity Reduction and Its Potential Application in Enhanced Oil Recovery. ACS omega. 2023;9(1):422-436. https://doi.org/10.1021/acsomega.3c0587

[19] Visan AI, Popescu-Pelin G, Socol G. Degradation behavior of polymers used as coating materials for drug delivery—A basic review. Polymers. 2021;13(8):1272. https://doi.org/10.3390/polym13081272

[20] Rajan R, Ahmed S, Sharma N, Kumar N, Debas A, Matsumura K. Review of the current state of protein aggregation inhibition from a materials chemistry perspective: special focus on polymeric materials. Materials Advances. 2021;2(4):1139-1176. https://doi.org/10.1039/D0MA00760A

[21] Meng R, Wang C, Jin J, Wang R, Deng L. Self-assembly of hydrophobically associating amphiphilic polymer with surfactant and its effect on nanoemulsion. Colloids and Surfaces A: Physicochemical and Engineering Aspects. 2022;642:128599. https://doi.org/10.1016/j.colsurfa.2022.128599

[22] Wang W, Lai X, Hong F, Yang W, Wang L, Song X, et al. Study on the Intermolecular Action Mechanism and Rheological Properties of A Surfactant-Modified Hydrophobic Copolymer. Journal of Applied Polymer Science. 2025:e58117. https://doi.org/10.1002/app.58117

[23] Guzik A, de Maere d'Aertrycke F, Stuart MC, Raffa P. Lowest gelation concentration in a complex-coacervate-driven self-assembly system, achieved by redox-RAFT synthesis of high molecular weight block polyelectrolytes. Soft Matter. 2024;20(44):8727-8741. https://doi.org/10.1039/D4SM00763H

[24] Lu W, Hong K, Mays J. New class of thermoplastic elastomers based on acrylic block copolymers. Advances in Thermoplastic Elastomers: Elsevier; 2024. p. 125-149. https://doi.org/10.1016/B978-0-323-91758-2.00006-4

[25] Nabiyan A, Max JB, Schacher FH. Double hydrophilic copolymers–synthetic approaches, architectural variety, and current application fields. Chemical Society Reviews. 2022;51(3):995-1044. https://doi.org/10.1039/D1CS00086A

[26] Kuperkar K, Patel D, Atanase LI, Bahadur P. Amphiphilic block copolymers: their structures, and self-assembly to polymeric micelles and polymersomes as drug delivery vehicles. Polymers. 2022;14(21):4702. https://doi.org/10.3390/polym14214702

[27] Aleid GM, Alshammari AS, Tripathy DB, Gupta A, Ahmad S. Polymeric surfactants: recent advancement in their synthesis, properties, and industrial applications. Macromolecular Chemistry and Physics. 2023;224(17):2300107. https://doi.org/10.1002/macp.202300107

[28] Breul K. Structure–Property Relationships of Responsive and Reversible Gels: Chemical Design of Covalent and Supramolecular Polymer Networks: Dissertation, Mainz, Johannes Gutenberg-Universität Mainz, 2022; 2021

[29] Ozowe W, Daramola GO, Ekemezie IO. Recent advances and challenges in gas injection techniques for enhanced oil recovery. Magna Scientia Advanced Research and Reviews. 2023;9(2):168-178. https://doi.org/10.30574/msarr.2023.9.2.0180

[30] Kudapa VK, Krishna KS. Heavy oil recovery using gas injection methods and its challenges and opportunities. Materials Today: Proceedings. 2024;102:247-256.

[31] Zhang P, Wang Y, Chen W, Yu H, Qi Z, Li K. Preparation and solution characteristics of a novel hydrophobically associating terpolymer for enhanced oil recovery. Journal of solution chemistry. 2011;40(3):447-457.

[32] Torres-Martínez JG, Pérez-Alvarez M, Jiménez-Regalado EJ, St Thomas C, Alonso-Martínez F. Behavior study of a thermo-responsive hydrophobically associative water-soluble terpolymer in laboratory test with heavy crude oil. Journal of Applied Polymer Science. 2022;139(36):e52860. https://doi.org/10.1002/app.5286

[33] Jinhua H, Siman Z, Junwei L, Chenxi W, Ruizhi Z, Xing Z, et al. Synthesis, investigation of temperature and salt resistant polyacrylamide microspheres used for deep sealing and profile control and function strengthening mechanism. Journal of Applied Polymer Science. 2024;141(27):e55620. https://doi.org/10.1002/app.55620

[34] Ye Z, Feng M, Gou S, Liu M, Huang Z, Liu T. Hydrophobically associating acrylamide-based copolymer for chemically enhanced oil recovery. Journal of Applied Polymer Science. 2013;130(4):2901-2911. https://doi.org/10.1002/app.39424

[35] Ghosh P, Mohanty KK. Study of Surfactant–Polymer Flooding in High-Temperature and High-Salinity Carbonate Rocks. Energy & Fuels. 2019;33(5):4130-4145. https://doi.org/10.1021/acs.energyfuels.9b00407

[36] Ahsani T, Tamsilian Y, Rezaei A. Molecular dynamic simulation and experimental study of wettability alteration by hydrolyzed polyacrylamide for enhanced oil recovery: A new finding for polymer flooding process. Journal of Petroleum Science and Engineering. 2021;196:108029. https://doi.org/10.1016/j.petrol.2020.108029

[37] Wang S, Xiong P, Liu X, Meng F, Ma Q, Song C, et al. A Hydroxypropyl Methyl Cellulose-Based Graft Copolymer with Excellent Thermothickening and Anti-salt Ability for Enhanced Oil Recovery. Energy & Fuels. 2022;36(5):2488-2502. https://doi.org/10.1021/acs.energyfuels.1c03699

[38] Lalehgani Z, Ramazani S.A. A, Tamsilian Y, Shirazi M. Inverse emulsion polymerization of triple monomers of acrylamide, maleic anhydride, and styrene to achieve highly hydrophilic–hydrophobic modified polyacrylamide. Journal of Applied Polymer Science. 2019;136(29):47753. https://doi.org/10.1002/app.47753

[39] Ahmed, S.K., Ali, W.B. & Khadom, A.A. Synthesis and investigations of heterocyclic compounds as corrosion inhibitors for mild steel in hydrochloric acid. Int J Ind Chem. 2019; 10, 159–173 https://doi.org/10.1007/s40090-019-0181-8

[40] Arthur, D.E., Jonathan, A., Ameh, P.O. *et al.* A review on the assessment of polymeric materials used as corrosion inhibitor of metals and alloys. Int J Ind Chem. 2013; 4(2) https://doi.org/10.1186/2228-5547-4-2